Waste Heat Recovery From The Hot Water Boiling Plant Analysis using CFD

D. D. Palande[1*], *N.C.Ghuge*[2], *Chetan R. Dapase*[3]

Department of Mechanical Engineering Matoshri college of Engineering & Research centre Nasik Maharastra India

dpalande@gmail.com[1],nilghuge@gmail.com[2], cdchets09@gmail.com[3]

Received 13 April, 2022; Revised 5 May, 2022; Accepted 5 May, 2022

Available online 6 May, 2022 at www.atlas-tjes.org, doi: 10.22545/2022/00182

To fulfill the world's growing need for fossil fuel energy, renewable energy harvesting is required, and the rate of depletion of non-renewable energy sources must be slowed. Currently, many of these techniques are available, but with less effectiveness than before. These techniques result in a long payback period of investment. The goal of this research is to look at many elements of convective heat transfer enhancement using finned heat pipes, as well as the recovery of industrial waste heat. To validate these new energy-saving concepts, ANSYS 2020 R1 is used, including control strategies and simulation techniques. An integrated waste heat recovery system using finned heat pipes is having a significant effect on overall efficiency. The efficiency is increased by 10.5%–18.8% for various load conditions.

Keywords: Finned heat pipe, Nusselt Number, Euler Number and convection.

1 Introduction

The energy crisis, brought on by a lack of oil and the rapid depletion of fossil fuels, draws attention to energy issues and leads to research into new and renewable energy sources, as well as a list of activities that must be undertaken to save energy. The country's economic development depends on energy conservation. Furnaces and heat equipment available in India have an efficiency of not more than 50%. This implies that the exhaust dissipates more than half of the energy created. A large quantity of fuel may be saved if this lost heat can be correctly captured. Waste heat is energy that is produced through the combustion of fuels or chemical reactions and then "dumped" into the atmosphere, despite the fact that it may still be employed for something useful and economically beneficial. A significant amount of primary fuel could be saved if some of this waste heat could be recovered. It is impossible to recover all of the energy lost in squandering gases. As a human being, it is the responsibility of every single person to save natural resources for the benefit of the next generation. As an engineer, it is the responsibility of every engineer to save any possible waste energy available in the industry and help the cause of saving natural resources. Because of the high cost of fuel, most Indian enterprises did not pay attention to the cost of fuel savings from recovered waste heat created in the sector two decades ago. In order to save fuel, it is important to retrieve heat from waste and reuse it in the process. With the goal of providing a user-friendly, efficient, and simple-to-operate system for extracting heat from waste, this project developed a highly efficient and static heat pipe based on a recovery system to convalesce any type of waste heat accessible in the industry and use it in the process to save fuel. Among the most effective waste heat recovery methods are heat exchangers built from heat pipes. A heat pipe has the advantage over all other methods. It can carry high volumes of heat over long distances with a compact design and no additional energy input.

Many researchers have worked on heat pipes and waste heat recovery. S.H. Noie-Baghban et al. [1] studied the design and heat transmission constraints of single heat pipes for three types of wick and three working fluids were explored in this study, which began with computer simulation. The minimum heat transfer rate for three working fluids (acetone, water, and methanol) was found to be significantly higher than the needed heat transfer rate. The heat exchanger's low efficiency (0.16) was attributed to the pipe's high pitch to diameter ratio and the lack of fins. Fabian Korn [2]examine the second key aspect: mass transport via porous medium due to vaporization and condensation. There are also capillary effects, pressure impacts, and heat conduction effects to consider, resulting in a complex heat transfer structure requiring a great deal of understanding. The study's goal was to design, build, and test a waste heat recovery system from a hot brass forging furnace using a heat pipe air-preheater. A mathematical model was built to forecast the heat transfer rate and was used to compute the heat pipe air-preheater. The heat pipe air-preheater can efficiently save energy by reducing the amount of gas used in the furnace. According to H. Hagens et al. [4], offered data and forecasting for a heat pipe exchanger with an R134a proportion of 19% and 59%. In relation to its diameter, the thermos-siphon is somewhat long. The rate of air fluctuated between 0.4 and 2.0 kg/s. The evaporator side of the heat pipe reached temperatures of 40 to 70 ˚C, while the condenser side reached temperatures of 20–50 ˚C. Timothy J. Rennie and colleagues [5] studied the laminar fluid flow and heat transfer characteristics of a double-pipe helical heat exchanger and were computationally modeled for different fluid flow rates and tube sizes. The heat transfer characteristics of a double-pipe helical heat exchanger for both parallel and counter flow were computationally studied using a computational fluid dynamics tool (PHOENICS 3.3). Validation runs were carried out with constant wall temperature and constant heat flux as boundary conditions. These simulations produced findings that were well within the range of those seen in the literature for helical coils. The goal of this research is to look at how geometric design affects the thermal performance of star-groove micro-heat pipes. Heat transport capacity improves as the cross-sectional area of the micro-heat pipe grows. The heat transfer capacity of the micro-heat pipe, on the other hand, decreases as the total length of the pipe increases. When the adiabatical section length is reduced but the overall length remains constant, the heat transport capacity increases. Ehsan Firouzfar et al. [7]This analysis of the use of heat pipe heat exchangers (HPHEs) in HVAC systems reveals that HPHEs are highly efficient heat transfer devices that may be simply deployed as thermal linkages and heat exchangers in air conditioning systems to save energy and protect the environment. T. Mallikharjuna Rao et al. [8] Thousands of condenser tubes are replaced by hundreds of "heat pipes" in this study. The material of the heat pipe, the length of the heat pipe, and the diameter of the heat pipe for condensation purposes are all detailed in detail.Zare Aliabadi et al. [9] studied the impact of several factors on the thermal performance of a gas-liquid HPHE. As Hussam Jouhara et al. [10] summarise, this research shows that increasing energy efficiency in industrial processes by utilizing waste heat recovery is possible using a variety of methodologies and state-of-the-art technologies. However, in order to achieve the highest possible efficiency for a system through waste heat recovery, the type of process in question should always be evaluated and analysed before a waste heat recovery method for energy efficiency optimization is assigned. Yiyu Men et al [12] studied the concept of further waste heat recovery is examined, and existing technologies are compared, as well as the waste heat potential and assessment index.Robert Stefan vizitiu et al[13] studied the efficiency improvement of heat pipe heat exchangers by using phase change material. From the above literature review, it is clear that for waste heat recovery purposes, the heat pipe heat exchanger is the best solution for the problem of waste heat recovery from hot water generation plants.

The objective of this study is to develop, manufacture, and assess a heat recovery system from a hot water boiler process employing a heat pipe air-preheater.

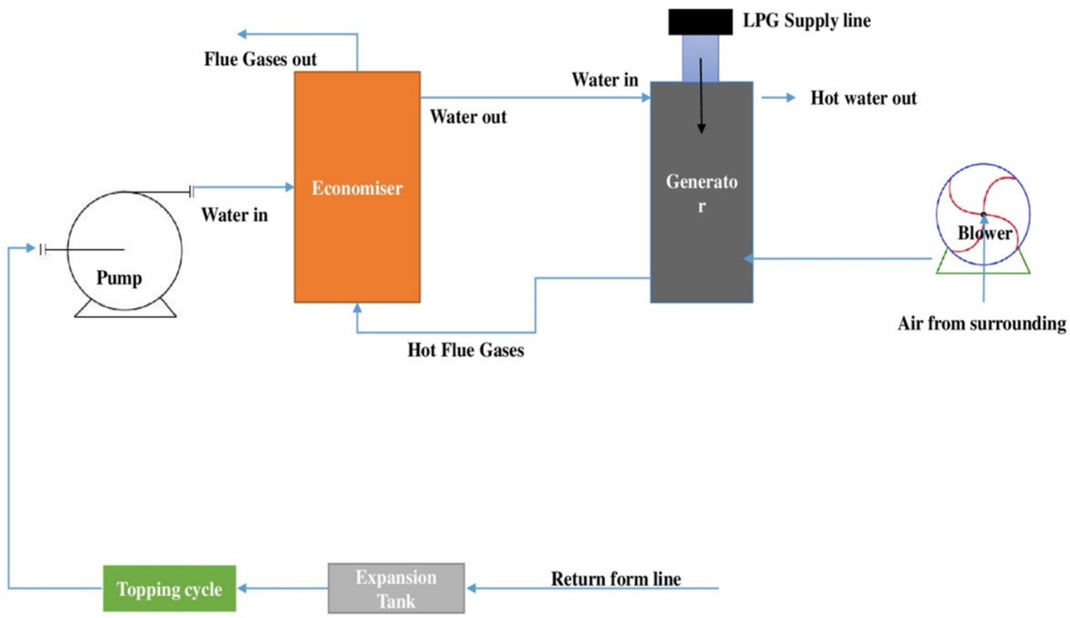

Figure 1: *Layout of system present condition.*

2 Potential of Waste Heat Revival in Industries

2.1 Waste Heat

Waste heat is additional energy that is expelled at a high temperature above normal air pressure from a system in order to obtain additional utility from it. According to the temperature range, waste heat systems are divided into two groups. They are waste heat with a high temperature range of more than 650 ˚C and waste heat with a low temperature range of less than 230 ˚C.

2.2 Present Working System

Figure 1 shows the present working of the hot water boiling plant. In this system, waste heat recovery is done at the end of the economizer where the flue gas temperature is 150 to 160 ˚C. Waste heat can be recovered by adding the heat pipe air-preheater at the end of the economizer, where the exhaust temperature is reduced by up to 65–75 ˚C. This heat is used to heat the atmospheric air, and this preheated air is supplied to the generator. This will result in saving the fuel supply system. The experiment's findings revealed that as the temperature of the hot gas grew, so did the rate of heat transmission. The heat pipe air-preheater can lower the amount of gas used in the boiler, resulting in significant energy savings. Using a heat recovery system at the exhaust of the economizer and supplying the preheated air to the blower again will help to improve boiler efficiency and save the Liquefied Petroleum Gas (LPG) fuel supply effectively.

Figure 2 shows the proposed system for the waste heat recovery from a hot water boiler plant where the heat pipe heat exchanger system is fixed at the outlet of the economizer for the cooling purpose of the flue exhaust gas and to heat the atmospheric air by passing air around the tubes. This preheated air is supplied to the generator, which helps to improve the efficiency of the generator as well as help consume the fuel supply.

Only pure liquid and vapor pass through heat pipes that run on a closed two-phase cycle. Until the operational temperature reaches between the triple point and the critical point, the working fluid stays saturated. Heat is delivered to the liquid via the shell when heat is transferred to the heat pipe's evaporator.

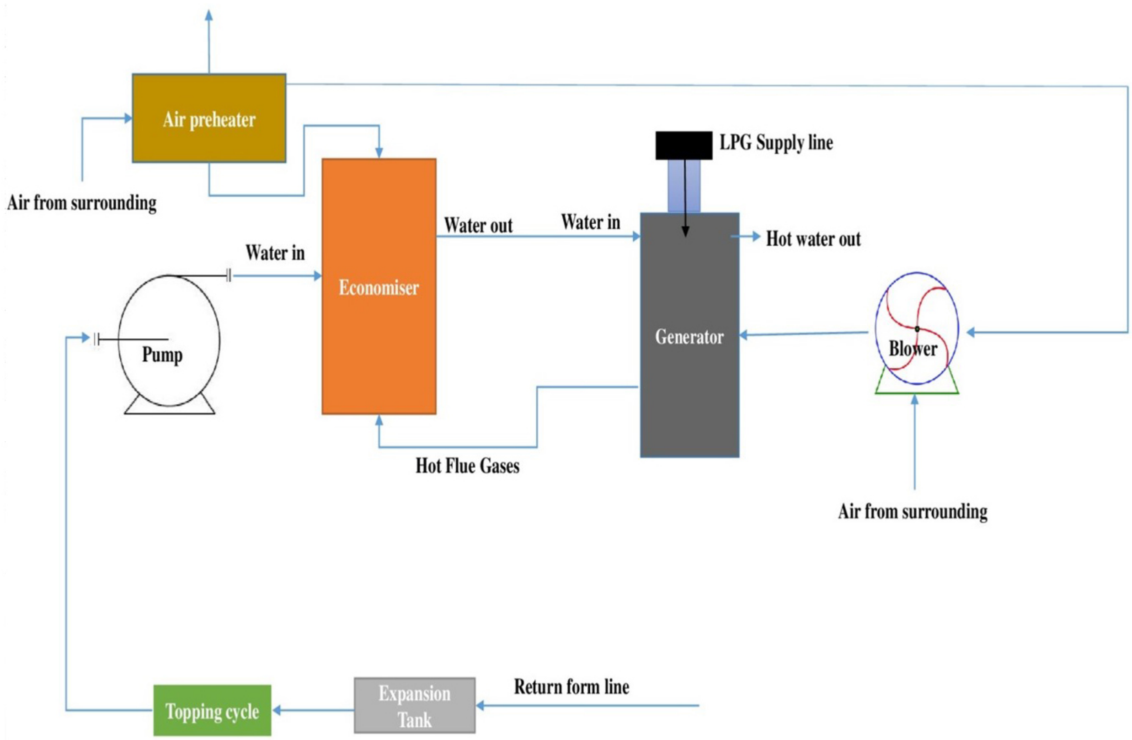

Figure 2: *Working system with heat pipe air-preheater.*

The liquid in the evaporator part vaporizes when it receives enough heat energy. The vapor transports thermal energy from the adiabatically to the cooling coil, in which it is cooled to liquid and the latent heat of evaporation is released. The condensate is knocked to the evaporator from the condenser by the liquid's driving force.

3 Description of Model

Figure 3(a) exhibits a model of the heat pipe generator [1], whereas Figure 3(b) depicts a real-life heat pipe heat exchanger. The parameters of an existing waste heat recovery system are shown in Table 1. The construction of the heat exchanger is the most expensive aspect of this work. It covers the costs of design, materials, and labor.

4 FEM analysis

In this work physical models of a heat exchanger with a single tube are used in this study. In the heat exchanger, a heat pipe is constructed, and a constant intake temperature for cold and hot fluid is selected. Inside the duct, a heat pipe is installed. Table 2 shows the size of heat exchangers. ANSYS was used to model the different heat pipe models. Figures 4 to 5 show the different aspects of the ANSYS FLUENT model of the heat exchangers.

Table 1: Experiment Result

Sr. No.	Hot Exhaust air from (Flue gas)	Unit	Qty
1	Volume of the flue gas	m^3/hr	1305
2	FLue gas Temperature (Exchanger inlet)	deg.c	140
3	Flue gas Temperature (Exchanger outlet)	deg.c	70
4	Temperature .difference	deg.c	70
5	Density of the flue gas at 140°C		0.963
6	Mass of the flue gas	kg/hr	1113.65
7	Possible energy recovery		18709.34
8	Type of system		air to air
9	Fuel used		LPG
10	Calorific value of the LPG	Kcal/kg	10000
11	Cost of the LPG	Rs	75
12	Working	hrs/day	20
13	Total working	Days	300

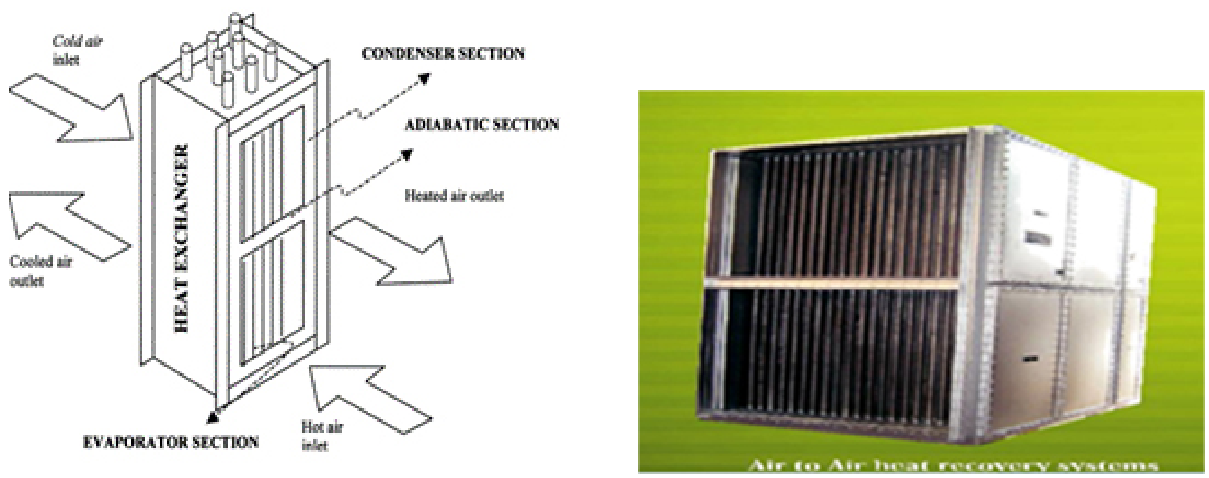

(a) (b)

Figure 3: (a) Representation of heat pipe heat exchanger [1], (b) Actual heat pipe heat exchanger.

Table 2: Dimensions of Duct

Dimensions	Value
Duct height	1400
Duct Width	400

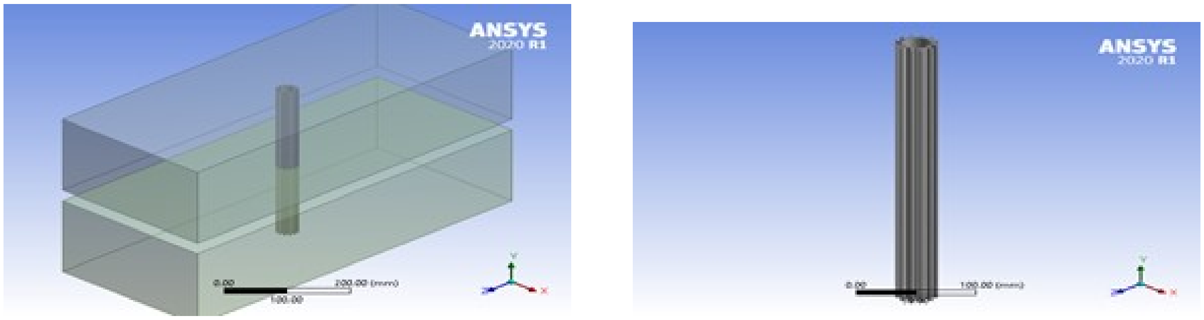

(a) **(b)**

Figure 4: (a) Heat exchanger model with single heat pipe, (b) Heat pipe model with finned surface.

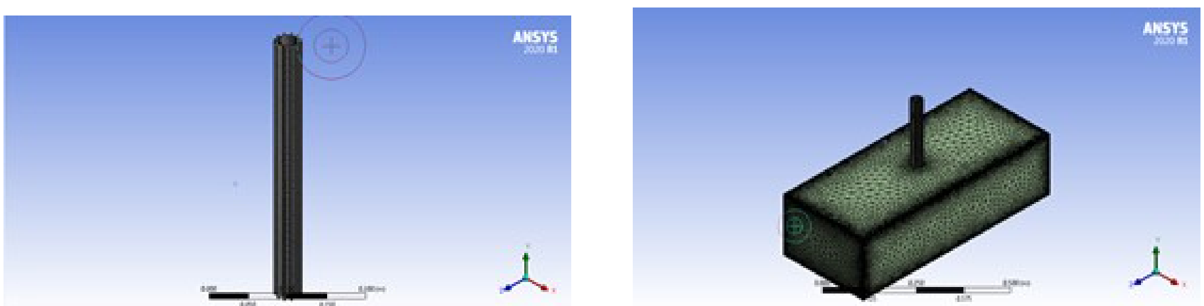

(a) **(b)**

Figure 5: (a) Heat pipe Model after grid independence study, (b) Heat pipe Model with Hot Fluid Domain with Fin meshing considering grid size after grid independence study.

4.1 Governing Equations

Steady, three dimensional turbulent, and incompressible flow is present in the tube. Turbulent models are selected based on the comparison of RNG $k-\varepsilon$ nd Realizable $k-\varepsilon$ models with Enhanced wall function. Since the accurate prediction of the adverse $k-\varepsilon$ (RKE) model is selected in the present work.

The basic governing equations (continuity, momentum, energy, turbulent kinetic energy (k), and dissipation of energy (ε) are

Continuity equation

$$\frac{\partial \rho}{\partial t} + \frac{\partial (\rho u)}{\partial x} + \frac{\partial (\rho v)}{\partial y} + \frac{\partial (\rho w)}{\partial z} = 0 \tag{1}$$

X-Momentum Equation

$$\rho \frac{Du}{Dt} = -\frac{\partial p}{\partial x} + \frac{\partial}{\partial x}\left[2\mu \frac{\partial u}{\partial x} + \lambda\, div\ u\right] + \frac{\partial}{\partial y}\left[\mu\left(\frac{\partial u}{\partial y} + \frac{\partial v}{\partial x}\right)\right] + \frac{\partial}{\partial z}\left[\mu\left(\frac{\partial u}{\partial z} + \frac{\partial w}{\partial x}\right)\right] + Smx \tag{2}$$

Y-Momentum Equation

$$\rho \frac{Dv}{Dt} = -\frac{\partial p}{\partial y} + \frac{\partial}{\partial x}\left[\mu\left(\frac{\partial u}{\partial y} + \frac{\partial v}{\partial x}\right)\right] + \frac{\partial}{\partial y}\left[2\mu \frac{\partial v}{\partial y} + \lambda\, div\ u\right] + \frac{\partial}{\partial z}\left[\mu\left(\frac{\partial v}{\partial z} + \frac{\partial w}{\partial y}\right)\right] + Smy \tag{3}$$

Z-Momentum Equation

$$\rho\frac{Dw}{Dt} = -\frac{\partial p}{\partial y} + \frac{\partial}{\partial x}\left[\mu\left(\frac{\partial u}{\partial z} + \frac{\partial w}{\partial x}\right)\right] + \frac{\partial}{\partial y}\left[\mu\left(\frac{\partial v}{\partial z} + \frac{\partial w}{\partial y}\right)\right] + \frac{\partial}{\partial z}\left[2\mu\frac{\partial w}{\partial y} + \lambda\, div\ u\right] + Smz \tag{4}$$

Energy Equation

$$\frac{\partial}{\partial t}(\rho E) + \frac{\partial}{\partial x_i}\left[u_i(\rho E + p)\right] = \frac{\partial}{\partial x_j}\left[\left(k_{eff}\frac{\partial T}{\partial x_i} + u_i(\tau_{ij})_{eff}\right)\right] + S_h \tag{5}$$

Where E is the total energy, k_{eff} is the effective thermal conductivity, and $(\tau_{ij})_{eff}$ is the deviatoric stress tensor.

Transport Equation of Turbulence:

The transport equations for the Realizable $k - \varepsilon$ turbulence model in the tensor form is given by:

$$\frac{\partial}{\partial t}(pk) + \frac{\partial}{\partial x_j}(pku_j) = \frac{\partial}{\partial x_j}\left[\left(\mu + \frac{\mu_t}{\sigma_k}\right)\frac{\partial k}{\partial x_j}\right] + G_k + G_b - \rho\varepsilon - Y_M + S_k \tag{6}$$

$$\frac{\partial}{\partial t}(p\varepsilon) + \frac{\partial}{\partial x_j}(p\varepsilon u_j) = \frac{\partial}{\partial x_j}\left[\left(\mu + \frac{\mu_t}{\sigma_\varepsilon}\right)\frac{\partial \varepsilon}{\partial x_j}\right] + \rho C_1 S\varepsilon + \rho C_2\frac{\varepsilon^2}{k + \sqrt{\vartheta\varepsilon}} + C_{1\varepsilon}\frac{\varepsilon}{k}C_{3\varepsilon}G_b + S_\varepsilon \tag{7}$$

$$C_1 = \max\left[0.43, \frac{\eta}{\eta + 5}\right], \eta = S\frac{k}{\varepsilon}, S = \sqrt{2S_{ij}S_{ij}} \tag{8}$$

In these equations, G_k represents the generation of turbulence kinetic energy due to the mean velocity gradients, calculated in modeling turbulent production in the $k - \varepsilon$ models. G_b is the generation of turbulence kinetic energy due to buoyancy in the effects of buoyancy on turbulence in the $k-\varepsilon$ models. Y_M represents the contribution of the fluctuating dilatation incompressible turbulence to the overall dissipation rate, in the effects of compressibility on turbulence in the $k - \varepsilon$ models. C_2 and $C_{1\varepsilon}$ are constants. σ_k and σ_ε are the turbulent Prandtl numbers for k and ε, respectively. S_k andS_ε are user-defined source terms.

$$\eta_t = \rho C_\mu\frac{\mu^2}{\varepsilon} \tag{9}$$

Is the turbulent viscosity and ε is the dissipation rate $\sigma_k, \sigma_\varepsilon, C_2, C_{1\varepsilon}$ and C_μ are the model constants with values of 1.0, 1.2, 1.9, 1.44 and 0.085, respectively.

In the present study, velocity inlet and pressure outlet boundary conditions are selected for the computational domain. The Uniform flow rate of cold air with a temperature of 298 K is assumed to be constant in the axial and radial direction and the uniform flow rate of hot flue gases with a temperature of 413 K is assumed to be constant in the axial and radial direction. A near-wall modeling approach can be done by employing the logarithmic law of the wall to estimate the kinetic energy and momentum at all rigid boundaries. FLUENT can combine the two-layer model with improved wall function. ANSYS FLUENT 2020 R1 is used to solve governing equations. A heat transfer between fluid and heat pipe is accepted even though it is negligible to understand the actual heat transfer phenomenon. The effect of gravity is considered. Thermo-physical properties of air and flue gases remain constant at the mean fluid temperature.

For Evaporation and condensation Equilibrium Model Equilibrium models are used to compute equilibrium ratios in Equation, The equilibrium models consider the case in which the species on the two phases are in dynamic equilibrium. The interphase mass transfer rate is determined from the relationship between the equilibrium species concentrations on the two phases. Typically at equilibrium the species concentrations on the two phases are not the same. However, there exists a well-defined equilibrium curve relating the two concentrations. For binary mixtures, the equilibrium curve depends on the temperature and pressure. For multi-component mixtures, it is also a function of the mixture composition. The equilibrium curve is usually monotonic and nonlinear, and is often expressed in terms of equilibrium mole fractions of species and on phases and

$$X^i_{q,e} = F\left(X^j_{p,e}\right) \tag{10}$$

The simplest curve or relationship is quasi-linear and assumes that at equilibrium the mole fractions of the species between the phases are in proportion:

$$X^i_{q,e} = K^X_{q^i p^j} X^j_{p,e} \tag{11}$$

4.2 Boundary Condition and Data Reduction

Required boundary conditions are assigned to the computational domain as the internal regions are assigned as fluid domains as they have common faces that are shared. The incompressible, Newtonian, turbulent, and 3D model is to be analyzed therefore velocity inlet boundary conditions and pressure outlet boundary conditions are used for this model. Constant temperature wall boundary conditions at the tube wall and coupled heat transfer boundary conditions are used in this 3D model.

It is required to analyze the performance of the given system based on heat transfer parameters and hydraulic parameters. For forced convective heat transfer following non-dimensional parameters are selected as follows.

Reynolds number

$$R_e = \frac{\rho V D}{\mu} \tag{12}$$

Nusselt Number

$$N_{u_{local}} = \frac{h_{local} \times D}{K_f} \tag{13}$$

Where is the h_{local} local convective heat transfer coefficient, and K_f is the thermal conductivity of the fluid. The area-averaged Nusselt number (Nu) can be calculated as:

Average Nusselt Number

$$N_u = \frac{1}{A}\int N_{u_{local}} \times dA \tag{14}$$

Where A is the heat transfer surface area.

4.3 Numerical Analysis

Ansys ICEM CFD 2020 R1 is used for meshing and grid generation. The new polyhedral unstructured grid is used near walls to get refined wall treatment and to understand near-wall velocity gradient phenomenon. To simulate the flow field and heat transfer rate through a fine relevance center with maximum and minimum size equal to (2mm) and high smoothing mesh near the wall to give Y $+ \leq 5$. Polyhedral mesh is prepared in FLUENT itself, this type of cell is a new grid technique that gives quicker convergence with less interaction, lower values of residual, robust convergence, and the solution runtimes can be faster than other mesh types with supplying the same computational results. Ansys 2020 R1 is used for numerical analysis and for solving governing equations using finite volume method (FVM). The SIMPLE algorithm is given by Patankar S.V.[11] is selected to solve the flow field while second-order upwind scheme is used for discretization of the momentum, energy, and turbulent equations to transact with the problem of pressure gradient and velocity. The convergence of solution is monitored based on Outlet temperature and convergence criteria. The solution is considered converged when all flow equation becomes less than 10^{-6} and Energy equation becomes less than 10^{-7}. The outlet temperature does not show any fluctuations with respect to iteration at these conditions.

4.4 Grid Independence Study

Grid size selection is important in numerical analysis as both computational time and the accuracy of the result are dependent on this parameter. Grid size can be varied by changing element size in meshing. Six different element sizes are chosen, which further gives six different grid sizes. 0.003m, 0.00275m, 0.0025m, 0.002m, 0.001m are selected and the corresponding grid sizes are 354847, 407568, 565029, 854875, 1054871, and 2654874 for grid independence study as shown in table 3. The Nusselt number and outlet temperature are selected for monitoring the changes in these parameters against changes in mesh elements. Deviations are in the range of 0.00388% to 1.46% for Nu, and 0.001150% to 5.46% for Tout.

Table 3: Grid Independence Study

Case	Mesh Element	Nu	% error	$T_{out(K)}$	% error
Case1	354847	28.97	-	324.20	-
Case2	407568	29.687	1.464	324.55	0.1082
Case3	565029	29.887	0.402	325.32	0.2366
Case4	854875	29.895	0.0160	325.33	0.0015
Case5	1054871	29.894	0.0045	325.33	0.0001
Case6	2654874	29.893	0.0038	325.33	0.00007

5 Result and Discussion

The results of heat transfer (Nusselt Number), outlet temperature of the cold fluid, and steam volume fraction are estimated. The following section explains different facts about all these output parameters.

5.1 Influence of the Inlet Temperature of Hot Fluid

In the heat, the Nusselt number increases due to the increase in hot fluid. Compared to a plane tube, a heat pipe-assisted heat exchanger increases the Nusselt number while increasing the Reynolds number and decreasing cold fluid inlet temperature. In a heat pipe, fluid in a core region remains less heated, while the fluid in the outer region gets heated. This causes flow circulation in the core region, which assists in the mixing of fluid to enhance heat transfer. This flow circulation depends on the heat transfer rate and temperature difference.

As the temperature difference decreases, heat transfer also decreases, and steam volume fraction also increases. In the present study, Nu and VOF are more in the core region where the strong vortex flow is produced, which interrupts the boundary layer development. This vortex flow causes mixed axial and tangential flow, resulting in more fluctuations in energy among fluid layers and, subsequently, the more thermal energy being transmitted into layers of fluid. This also causes separate vortex flow regions in between the core and the near-wall region, as shown in Figure 6(a). This can be explained by the secondary phase caused in the middle region, which allows flow mixing of two separate vortex flows in two regions in Fgure 6(b).Turbulent kinetic energy (TKE) contours show maximum TKE in the evaporation region.

It is also noted that the fluid flow caused by evaporation fluid transportation rate increases with a significant temperature difference. Also, the heat transfer rate is dependent on these criteria regarding fluid transportation. As shown in Figures 7(a). and 7(b)., the velocity of fluid in the cold region is higher, so the heat recovery process can be improvised significantly in this region. In spite of the vapor state of the fluid, the heat transfer rate is more due to this random motion of the fluid.

As revealed in Figures. 8(a) and 8(b), the heat transfer rate is greater in the near wall region as compared to the far wall region. As a result, the temperature difference is greater in this region, which causes a sudden rise in the heat content of fluid in that region and will cause the formation of fluid vapours

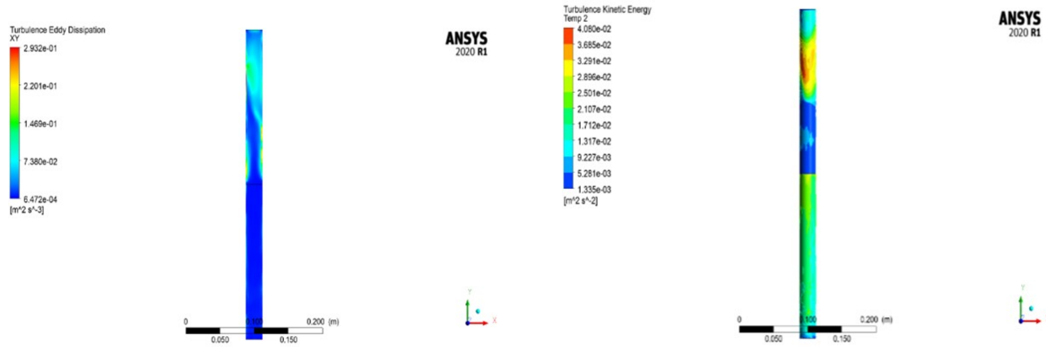

(a) **(b)**

Figure 6: (a) Turbulent eddy dissipation (TED) evaporation region, (b) Turbulent Kinetic Energy (TKE) evaporation region.

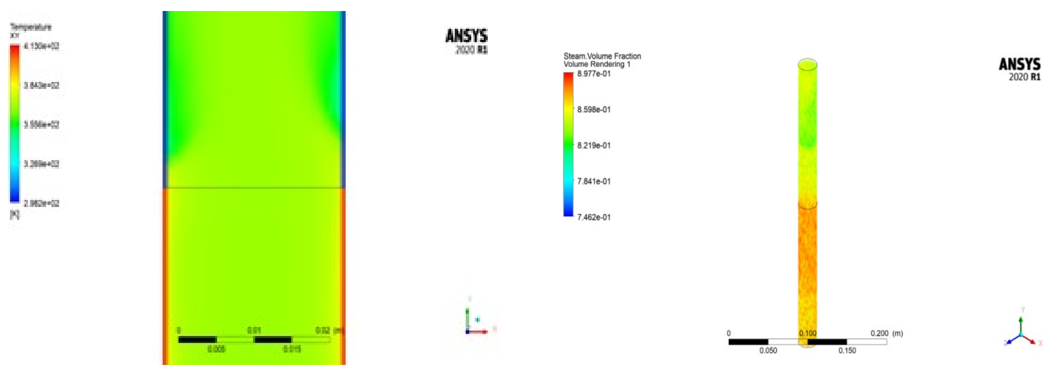

(a) **(b)**

Figure 7: (a) Near wall temperature of the hot region and cold fluid, (b) Steam Volume fraction in core region.

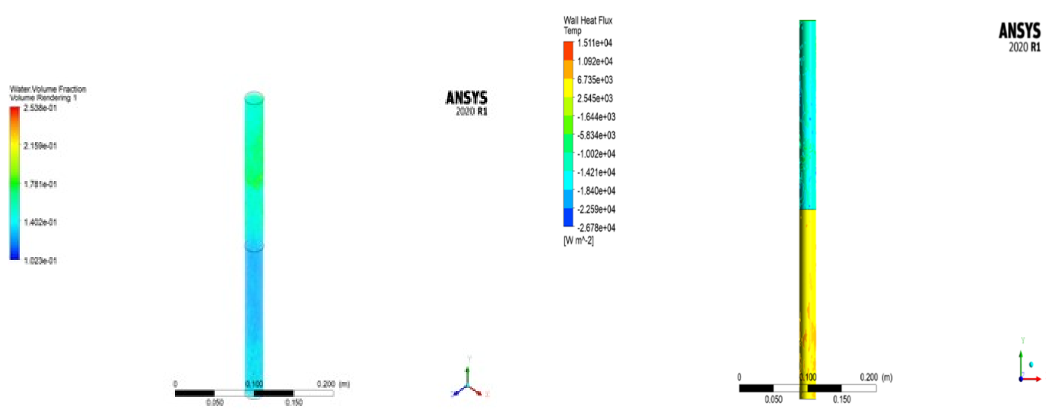

(a) **(b)**

Figure 8: (a) Water volume fraction in core region, (b) Heat transfer rate from hot region and cold region.

in this region. As shown in Figure. 8(a), it is needed to consider the fact that the rate of evaporation is an important parameter in the case of heat transfer from a heated liquid to cooled fluid.

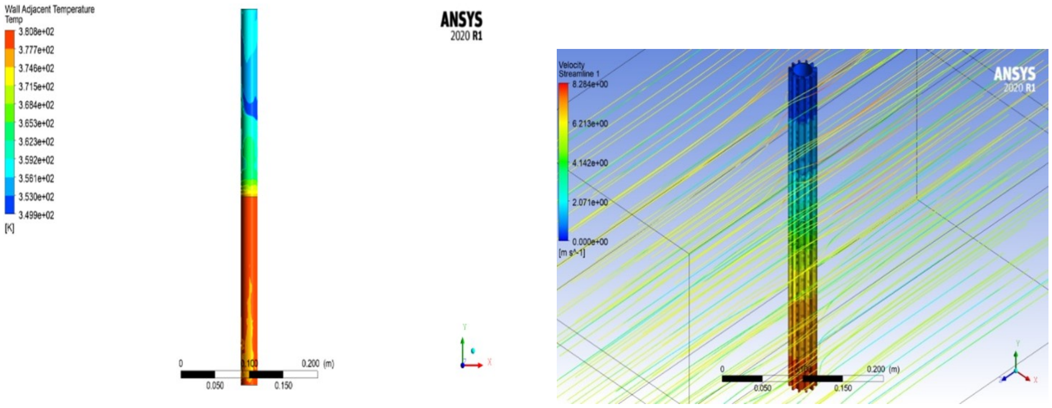

(a) **(b)**

Figure 9: (a) Temperature contour of heat pipe during heat transfer, (b) Air flow across finned heat pipe for heat transfer from hot fluid to cold fluid.

5.2 Effect of Steam Volume Fraction on Heat Transfer Rate

As the fluid gets evaporated, the volume fraction of steam increases. This rise in volume fraction indicates the evaporation process, and this is an important part of this heat transfer process. As this heat transfer increases with continuous evaporation of fluid in the hot fluid region and condensation in the cold fluid region, there is the formation of a mixture of liquid and vapor in the core region.

The rate of condensation in the cold region is less as compared to the evaporation rate as the heat transfer rate in the cold region is greater as the vapor form of fluid causes dissipation of heat more quickly than liquid fluid in the hot region of the heat pipe as shown in Figures 9(a) and 9(b). The temperature contour and air flow across the heat pipe are shown in Figure10(a) and 10(b) The heat transfer rate in a hot region is 172.49 w/m^2 and in a cold region is 282.98 w/m^2.The heat transfer coefficient of fluid in a cold region is found to be 30.06 w/m^{2}K and that of hot fluid is 30.48 w/m^{2}K.

5.3 Impact of Heat Pipe on Heat Exchanger

The occurrence of a combined evaporation and condensation action of fluid in the heat pipe allows heat transfer from hot to the cold fluid. Hot fluid with a velocity of 5.13m/s is passing over the heat pipe and as the fluid is cold at high pressure, it takes continuous heat from the hot fluid and gets evaporated, and then it transfers its heat to the cold fluid which is passing over the upper portion of the heat pipe. As the cold fluid has a velocity of 6.13m/s, it gains heat from the evaporated vapors of fluid inside the heat pipe.

This heat loss from vapors causes condensation of the vapors and gets accumulated at near-wall locations of the heat pipe where film-wise or drop-wise condensation will occur. This condensate was then collected in the lower portion of the heat pipe for further evaporation and condensation. As depicted in Figures 10(a) and 10(b), cold and hot fluids move through the heat pipe, causing the fluid inside the heat exchanger to be heated and cooled simultaneously. Consider a graphic with varying wall temperatures nearby to demonstrate this. The concept of heat exchange from hot to cold fluid as the temperature differential can be used to figure out how well heat exchangers work, as shown in Figures 11(a) and 11(b). The heat transfer also depends on the fluid flow parameters like velocity and pressure of the fluid passing over the finned heat pipe.

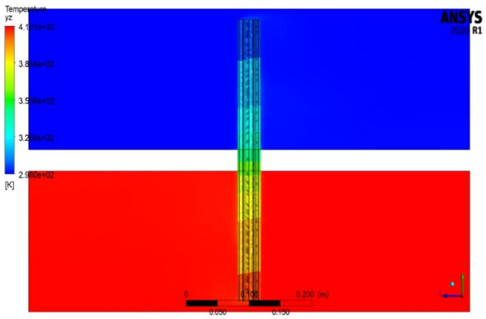

(a)

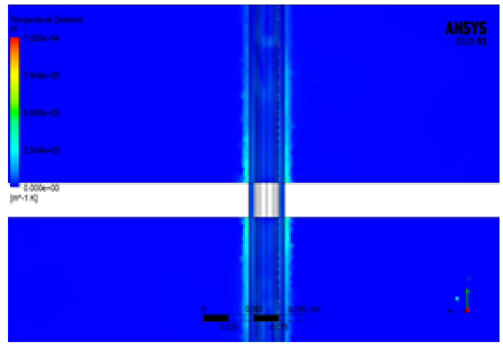

(b)

Figure 10: (a) Performance of heat pipe in heat exchanger, (b) All adjacent temperature gradient.

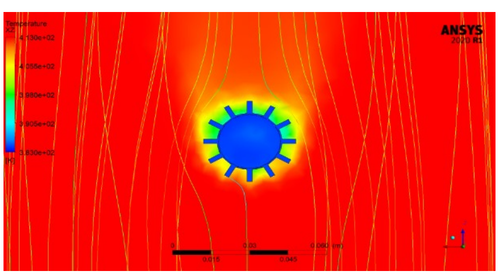

(a)

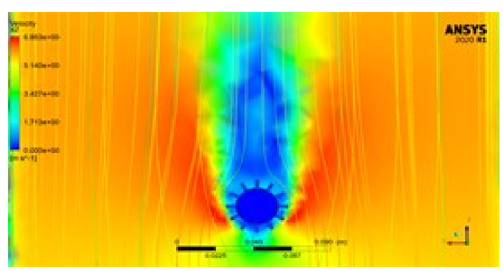

(b)

Figure 11: (a) Temperature contours across finned heat pipe in hot fluid region, (b) Velocity contours across finned heat pipe in hot fluid region.

6 Conclusion

The heat pipe provides a substantial increase in heat transfer while keeping pressure drop to a minimum. Although dimensionless parameters for heat transfer (Nu) and pressure drop (Δp) are very important for the scaling of the results of the heat exchanger with similar geometries, comparison of the performances of different heat transfer surfaces. Heat transfer and pressure drop compared with enhanced surfaces about 14% - 18%. Despite the pressure drop, fins had a considerable influence on the heat transfer increase in the overheated pipe. Heat transmission is increased by 10% to 15%. This increases by 10% when using a heat pipe. The basic results showed that Nusselt number and pressure drop were more effective than active heat transfer enhancement techniques. It is a cheap technique. It improves the heat transfer rate. While dimensionless heat transfer number (Nu) and pressure drop (p) characteristics are important for scaling heat exchanger findings with similar geometries, they don't provide a way to compare the performance of different heat transfer surfaces. Instead, comparing performance using such metrics will give the erroneous impression that non-enhanced (bare) surfaces are more efficient in terms of heat transfer and pressure drop. Heat transfer rate increases with increasing Reynolds number for all pin fin arrangements, but there is a significant difference between Reynolds number and flow rate due to flow reversal and continuous turbulence generation caused by the pin fin. The use of heat exchangers with heat pipes in an Integrated Waste Heat Recovery System has a substantial impact on the power plant's overall efficiency. This is due to the utilization of more space available in power plants, and this can enhance the effective heating of the water supplied to the economizer and any other utility.

Funding: This research received no external funding.

Conflicts of Interest: The authors declares no conflict of interest.

Authors Contributions: Co-authors contributed equally.

References

[1] S.H. Noie-Baghban, G.R. Majideian, (2000). Waste heat recovery using heat pipe heat exchanger (HPHE) for surgery rooms in hospitals. *Applied Thermal Engineering*, (20) 1271-1282.

[2] Fabian Korn,(2008). Heat pipes and its applications. 2008MVK160 *Heat and Mass Transport,* Sweden.

[3] Lerchai Yodrak, Sampan Rittidech,(2010). Waste heat recovery by heat pipe Aar-preheater to energy thrift from the furnace in a hot boiling process. *American Journal of Applied Sciences*, 7 (5): 675-681.

[4] H. Hagens, F.L.A. Ganzevles,(2007). Air heat exchangers with long heat pipes: Experiments and predictions. *Applied Thermal Engineering*, (27) 2426–2434.

[5] Timothy J. Rennie, Vijaya G.S. Raghavan (2006). Numerical studies of a double-pipe helical heat exchanger. *Applied Thermal Engineering*, (26) 1266–1273.

[6] Yew Mun Hung, Q'bert Seng(2011). Effects of geometric design on thermal performance of star-groove micro-heat pipes. *International Journal of Heat and Mass Transfer*, (54) 1198–1209.

[7] Ehsan Firouzfar, Mohammad Soltanieh(2011). Application of heat pipe heat exchangers in heating, ventilation and air conditioning (HVAC) systems. *Scientific Research and Essays*, Vol. 6(9) 1900-1908.

[8] T. Mallikharjuna Rao (2014). Heat pipes for steam condensation. *IOSR Journal of Mechanical and Civil Engineering*, (IOSR-JMCE) Vol.11(2) 16-19.

[9] H. Zare Aliabadi, H. Ateshi (2009). An experimental and theoretical investigation on thermal performance of a gas-liquid thermosyphon heat pipe heat exchanger in a semi-industrial plant. *Iranian Journal of Chemical Engineering*, Vol. 6(3) 13-25.

[10] Hussam Jouhara, Navid Khordehgah, Sulaiman Almahmoud, Bertrand Delpech, Amisha Chauhan, avvas A. Tassou(2018). Waste heat recovery technologies and applications. *Thermal Science and Engineering Progress*, (6) 268–289.

[11] Patankar S.V (1980). *Numerical heat transfer and fluid flow*. Taylor and Francis.

[12] Yiyu Men, Xiaohua Liu,Tao Zhang (2021). A review of boiler waste heat recovery technologies in the mediumlow temperature range. *Energy*, (237) 121560.

[13] Robert Stefan vizitiu et al (2019). CFD analysis of an innovative heat recovery system. *Procedia Manufacturing*, (32) pp 488–495.

About the Authors

Dr.D.D.Palande is currently working as an Associate Professor in the Mechanical Engineering Department at Matoshri College of Engineering and Research center Nasik. He is B.E (Mechanical) M.E.(Thermal Power Engineering) and Ph.D. (Mechanical Engineering). He is having 21 years of experience in teaching and administration. He is a member of Professional Societies such as the Institution of Engineers (India), and the Indian Society for Technical Education (ISTE). He has published many research papers in various national and international Journals.

Dr.Nilesh C. Ghuge is currently working as an Associate Professor in the Mechanical Engineering Department at Matoshri College of Engineering and Research center Nasik. He is B.E (Mechanical) M.E.(Mechanical Engineering) and Ph.D. (Mechanical Engineering). He is a member of Professional Societies such as the Institution of Engineers (India), the Indian Society for Technical Education (ISTE), He is having 22 years of experience in Industry and teaching and administration. He has published many research papers in various national and international Journals.

Mr. Chetan Dapase has completed M.E.(Heat Power Engineering). He is having 10 years of experience in the Industry. Currently he is working as director of Gayatri Enterprises at Nasik.(M.S.).